ELSEVIER

Cement & Concrete Composites 21 (1999) 301–312

Cement & Concrete Composites

Mechanical behaviour of ferrocement composites: an experimental investigation

Mohammed Arif [a], Pankaj [b,*], Surendra K. Kaushik [c]

[a] Department of Civil Engineering, Aligarh Muslim University, Aligarh 202 002, India

[b] School of Civil and Environmental Engineering, The University of Edinburgh, Division of Engineering, Crew Building, Edinburgh EH9 3JN, Scotland, UK

[c] Department of Civil Engineering, University of Roorkee, Roorkee 247 667, India

Received 12 January 1998; accepted 26 February 1999

Abstract

In-plane tension, compression and bending tests were conducted on plain mortar and ferrocement specimens with woven and welded meshes. Tension tests were also carried out on meshes. Bending tests were conducted using specimens with centre point loading. The objective of the study was to investigate the behaviour of material reinforced with varying number of mesh layers and orientations and to evolve a set of elastic and inelastic material properties. It is observed that the conventional empirical relations based on mortar crushing strength overestimate the mortar modulus. The elastic moduli obtained using the rule of mixtures compares well with the values evaluated from the tests on ferrocement specimens. The 45° orientation emerges as the weakest configuration both in terms of the Young's modulus and ultimate stress because of the lowest volume fraction of wire mesh in the direction of loading at this orientation. © 1999 Elsevier Science Ltd. All rights reserved.

Keywords: In-plane tension and compression tests; Flexural tests; Mesh layers and orientations; Mortar modulus; Rule of mixtures

1. Introduction

Experimental investigations to study the mechanical behaviour of ferrocement have been going on since late fifties [1]. A number of experimental programmes that involved testing of ferrocement specimens under tension, compression or flexure were undertaken by various investigators e.g. [2–6] with diverse objectives. Some of these, for example, were designed to evaluate the variation in ultimate strength due to changes in geometry and orientation of reinforcing meshes [2,3]. The importance of these parameters arose from the reason that standard ultimate load analysis made no provision for steel oblique or perpendicular to the direction of applied stresses. Some other experimental programmes were aimed at examining the serviceability limit states of ferrocement. For example, Balaguru, Naaman and Shah [4] focused on the quantitative evaluation of deflection, crack distribution and crack widths of ferrocement in flexure. They evolved a mathematical model to predict load–deflection and moment-curvature response of ferrocement specimens in flexure.

The primary intent of the experimental programme discussed here was to evolve a set of material properties that can be subsequently used to analytically simulate the mechanical behaviour of ferrocement under a wide range of loading conditions. Analytical simulations [7] have, however, not been included in this paper. The experimental programme included testing of ferrocement specimens in tension, compression and flexure. Similar specimens of mortar were also tested in tension, compression and flexure. Two types of wire meshes viz. woven and welded were used. Tests to evaluate the properties of the wire meshes in tension were also conducted. In ferrocement specimens the number of wire mesh layers and their orientations were varied. The programme was expected to relate the elastic modulus of ferrocement to that of its constituents and the effect of mesh orientation on elastic modulus and yield stresses of ferrocement. Each test was conducted at least three times with identical specimens. Load–displacement plots

* Corresponding author. Tel.: +44 131 650 5800; fax: +44 131 650 6781; e-mail: Pankaj@ed.ac.uk

0958-9465/99/$ – see front matter © 1999 Elsevier Science Ltd. All rights reserved.
PII: S0958-9465(99)00011-6

were smoothened using a second degree polynomial and data from all tests of that category. The second degree polynomial was found to yield satisfactory results. The evolved properties have been tabulated in detail. These properties were derived from the raw data and not from the smoothened curves.

2. Constituent materials

Cement, sand, metallic wire meshes and water were used for casting mortar and ferrocement specimens. Ordinary Portland cement conforming to Indian Standard Specification IS: 269-1989 [8] was used throughout this investigation. The mix proportion for the cement sand mortar was 1:2.5 by weight with a water cement ratio of 0.45.

Machine woven galvanised steel wire mesh of opening size 7.5×6.0 mm with an average wire diameter of 0.72 mm and welded square galvanised steel wire mesh of opening size 15×15 mm with an average diameter of 1.44 mm were used.

3. Casting of test specimens

To evaluate the mechanical properties for each mesh, three specimens were cast. The ends of the meshes were embedded in a mortar pad in the manner prescribed by ACI 549.1R-88 [9].

For the casting of mortar and ferrocement specimens, wooden moulds made of boiling water proof ply sheets, were used. These sheets were cut along the width to facilitate demoulding. The sheets were positioned using metallic strips and fastened by bolts for the required thickness (Fig. 1). The mesh layers were cut to size and laid in between the mortar layers thus providing a clear cover of 4 mm on both the top and bottom faces. For the in-plane tests in order to achieve an appropriate grip, the grip portion of the samples was kept wider than the central region of the sample (Fig. 2(a)), whereas for specimens for flexural tests these were of uniform width (Fig. 2(b)). These samples were demoulded after 24 h and cured under wet gunny bags for 28 days. The details of the cast specimens of different categories are listed in Table 1. The thickness of the test specimens for in-plane and flexural tests was decided as per the accepted codal norms [9] whereas the width and length of the specimens were selected taking into account the limitations imposed by the testing machine.

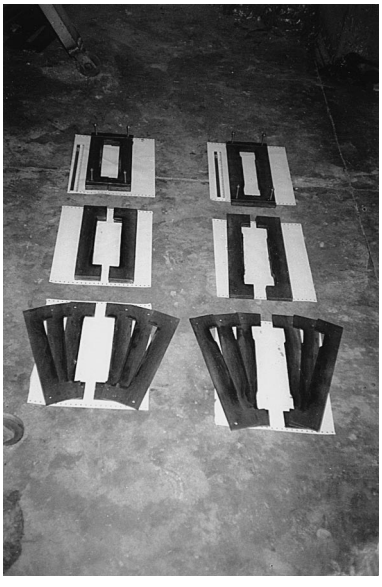

Fig. 1. Mould for casting specimens.

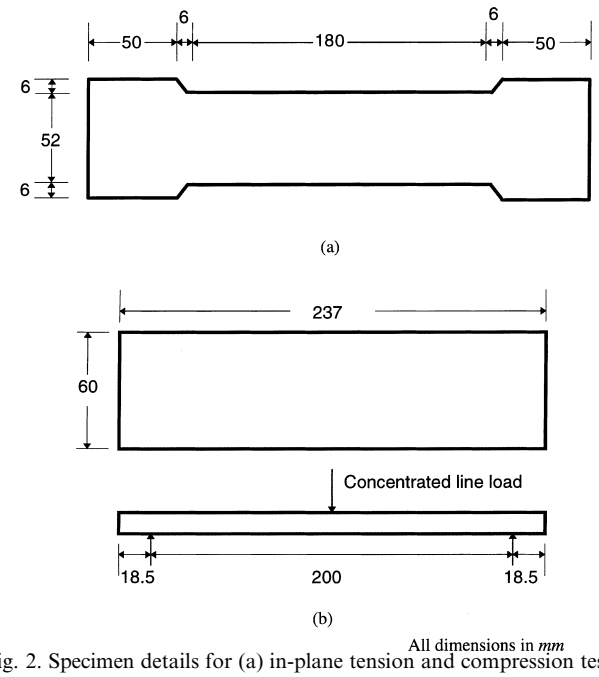

Fig. 2. Specimen details for (a) in-plane tension and compression tests and (b) flexural tests.

4. Tests on specimens

4.1. Wire meshes

Tests on wire mesh samples were carried out in the manner prescribed by ACI 549.1R-88 [9]. The tensile tests on the specimens were carried out on INSTRON Universal Testing Machine (Model 1342) under controlled displacement condition. The rate of displacement was kept as 0.5 mm/min.

Table 1
Details of specimens for in-plane tension, compression and flexural tests

Material	Tested for	Category designation	Dimensions (mm)	Mesh type	No. of mesh layers	Mesh orientation
Mortar	Tension	T4	182 × 52 × 19			
		T5	182 × 52 × 24			
		T6	182 × 52 × 29			
	Compression	C4	182 × 52 × 19			
	Flexure	F2	237 × 60 × 9			
		F3	237 × 60 × 14			
		F4	237 × 60 × 19			
		F5	237 × 60 × 24			
		F6	237 × 60 × 29			
Ferrocement in woven mesh	Tension	T3WN00	182 × 52 × 24	Woven	3	0°
		T3WN15	182 × 52 × 24	Woven	3	15°
		T3WN30	182 × 52 × 24	Woven	3	30°
		T3WN45	182 × 52 × 24	Woven	3	45°
		T3WN60	182 × 52 × 24	Woven	3	60°
		T3WN75	182 × 52 × 24	Woven	3	75°
		T3WN90	182 × 52 × 24	Woven	3	90°
		T4WN00	182 × 52 × 30	Woven	4	0°
		T5WN00	182 × 52 × 36	Woven	5	0°
	Compression	C3WN00	182 × 52 × 24	Woven	3	0°
Ferrocement in welded mesh	Tension	T3WL00	182 × 52 × 24	Welded	3	0°
		T3WL30	182 × 52 × 24	Welded	3	30°
		T3WL45	182 × 52 × 24	Welded	3	45°
		T3WL60	182 × 52 × 24	Welded	3	60°
		T3WL90	182 × 52 × 24	Welded	3	90°
Ferrocement in woven mesh	Flexure	F3WN00	237 × 60 × 24	Woven	3	0°
		F3WN30	237 × 60 × 24	Woven	3	30°
		F3WN45	237 × 60 × 24	Woven	3	45°
		F3WN60	237 × 60 × 24	Woven	3	60°
		F3WN90	237 × 60 × 24	Woven	3	90°
		F4WN00	237 × 60 × 30	Woven	4	0°
		F5WN00	237 × 60 × 36	Woven	5	0°
Ferrocement in welded mesh	Flexure	F3WL00	237 × 60 × 24	Welded	3	0°
		F3WL30	237 × 60 × 24	Welded	3	30°
		F3WL45	237 × 60 × 24	Welded	3	45°
		F3WL60	237 × 60 × 24	Welded	3	60°
		F3WL90	237 × 60 × 24	Welded	3	90°

4.2. Mortar

Mortar specimens for tension tests were prepared in thickness of 19, 24 and 29 mm as listed in Table 1. These samples were tested under controlled displacement condition at a rate of 0.5 mm/min. The machine was capable of generating reliable load–displacement data. Electrical resistance strain gauge rosettes were also pasted at the centre of the specimens to record strains in longitudinal and transverse directions. Unfortunately the results obtained from the latter were found to be unreliable and had to be ignored. Specimens for compression tests were 19 mm thick and once again tested under a controlled displacement rate of 0.5 mm/min. Mortar specimens for flexural tests were prepared in thickness of 9, 14, 19, 24 and 29 mm. The specimens were simply supported at the ends leaving an overhang of about 2 cm at each end (Fig. 2(b)). The concentrated line load was applied at the centre (Fig. 3).

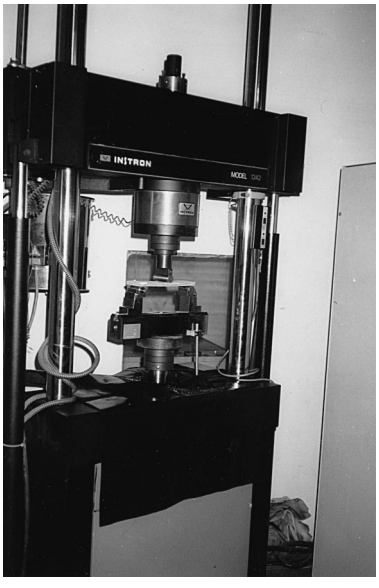

Fig. 3. Testing of specimens under flexure.

4.3. Ferrocement

Ferrocement specimens prepared for tension, compression and flexural tests are also listed in Table 1. In each category a minimum of three samples were tested. In tension tests, for samples with woven mesh at 0° orientation, the number of mesh layers was also varied. The ferrocement specimens tested under tension are shown in Fig. 4. Compression tests on ferrocement specimens were conducted only on specimens with woven mesh in 3 layers and at 0° orientation. One of the tested specimens is shown in Fig. 5. The number of mesh layers was also varied in flexural tests for samples with woven mesh at 0° orientation. The support conditions and the test procedure was the same as described for mortar specimens tested under flexure. The tested specimens are shown in Fig. 6.

5. Tests results and discussion

5.1. Cement sand mortar

The fineness modulus for the sand was determined using the sieve analysis data as 2.80. The density of loose sand was 12.86 kN/m^3 and compacted sand 13.97 kN/m^3. The average strength properties for the cement sand mortar obtained from the tests were as given in Table 2. These properties satisfy the strength requirements of Indian Standard Code IS: 456-1978 [10].

Fig. 4. Ferrocement specimens tested under in-plane tension.

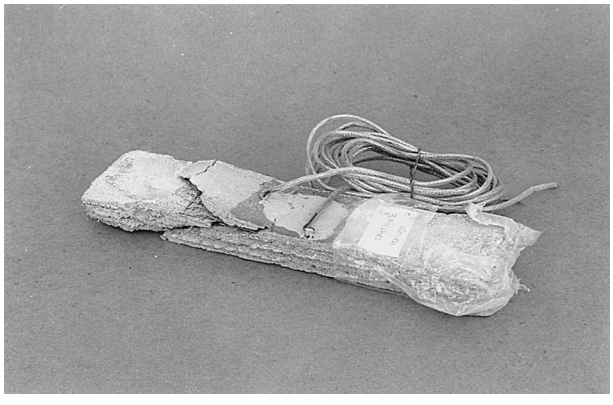

Fig. 5. Ferrocement specimens tested under in-plane compression.

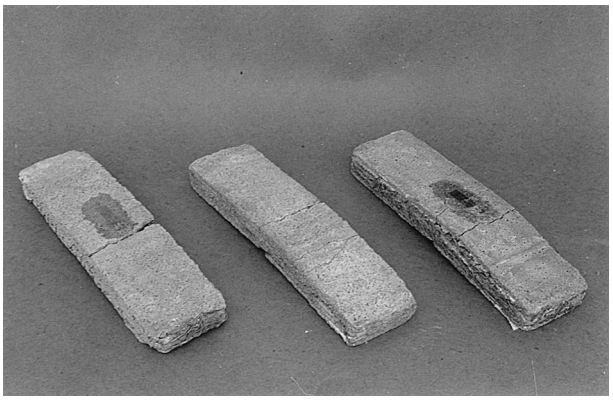

Fig. 6. Ferrocement specimens tested under flexure, with tension faces upward.

5.2. Wire meshes

The load–displacement curves for the woven and welded meshes and the corresponding average stress–strain curves are shown in Fig. 7. The sudden drop of load in Fig. 7(a) corresponds to the snapping of the longitudinal wires. Therefore, the figure indicates that different wire strands reach their snapping load at different instances of time. This can be attributed to the weave effect and variations in geometrical and material properties. This effect was more predominant in woven meshes (Fig. 7(a)). The stress at the first yield, ultimate tensile stress and the modulus of elasticity of the meshes deduced from the load–displacement data are given in Table 3.

5.3. Mortar under in-plane tension

The average load–displacement plots are shown in Fig. 8. The figures indicate a decline of load carrying capacity prior to failure. With the increasing load a transverse crack was observed across the mid section. This crack widened as the load was increased, leading to

Table 2
Strength properties of mortar

Average compressive strength of 100 × 100 × 100 mm cubes	19.5 MPa
Average compressive strength of 75 × 150 mm cylinders	18.2 MPa
Average tensile strength from briquettes	2.7 MPa

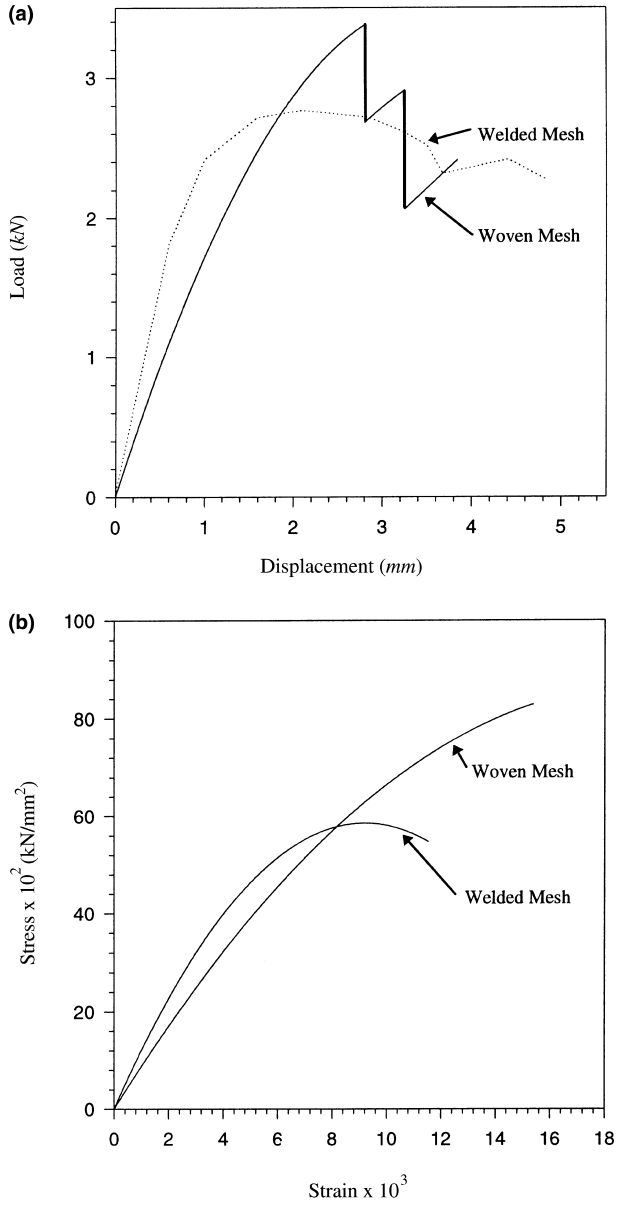

Fig. 7. (a) Load–displacement and (b) stress–strain curve for woven and welded wire meshes.

the subsequent failure of the specimens along a single well defined crack. In some cases a number of transverse micro-cracks were also observed during loading. However, sudden brittle failure with a single crack orthogonal to the loading direction occurred in all specimens. From the tension tests performed, properties of mortar in tension as shown in Table 4 were derived. In the evaluation of the Young's modulus, transverse stresses were ignored. This would obviously result in a slight overestimation of the modulus. The ultimate stress in this and subsequent tables corresponds to the peak load carried by the specimens.

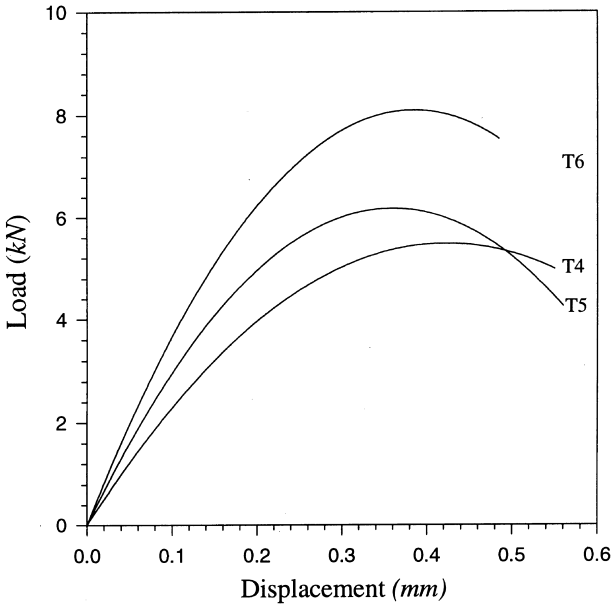

Fig. 8. Load–displacement curves for mortar specimens under in-plane tension.

5.4. Mortar under in-plane compression

The average load–displacement plot for mortar under compression is shown in Fig. 9. It can be seen that in

Table 4
Properties of mortar under in-plane tension

Category designation	T4	T5	T6	Average
Elastic modulus (MPa)	4981	5180	5050	5070
Stress at first deviation from linearity (MPa)	2.74	2.85	2.78	2.79
Ultimate stress (MPa)	5.25	5.4	5.2	5.28
Strain at failure	0.0030	0.0032	0.0031	0.0031

Table 3
Properties of wire mesh

S. No.	Particulars	Stress at first yield (MPa)	Ultimate tensile stress (MPa)	Modulus of Elasticity (MPa)
1.	Machine woven galvanised mesh with opening size 7.5 × 6.0 mm and average wire diameter of 0.72 mm	295	835	89 312
2.	Welded square galvanised mesh with opening size 15 × 15 mm and average wire diameter of 1.44 mm	307	563	1 11 641

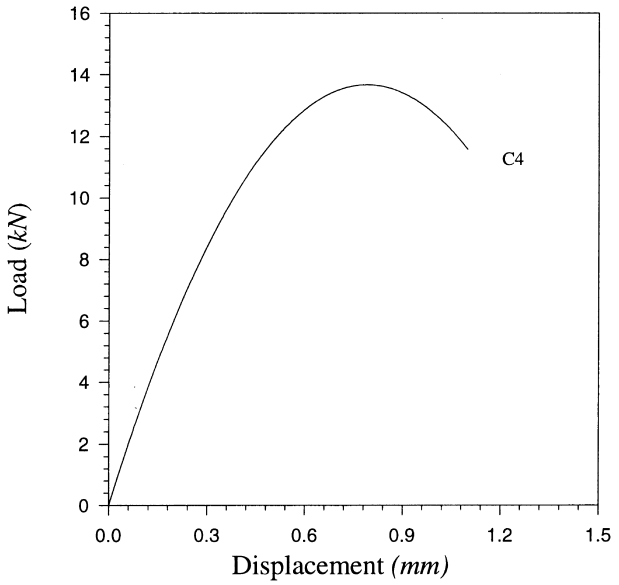

Fig. 9. Load–displacement curve for mortar specimens under in-plane compression.

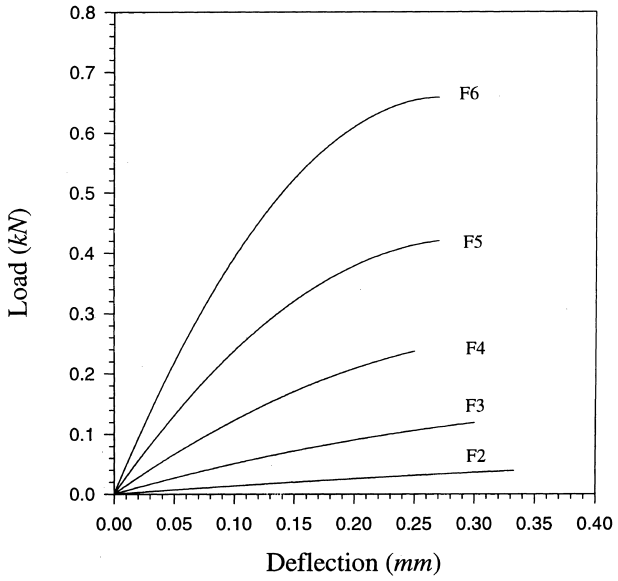

Fig. 10. Load–deflection curves for mortar specimens under flexure.

this case as well a drop in the load carrying capacity occurs prior to failure. With increasing loads, longitudinal cracks developed along the mid section. As the loads were increased the cracks widened and spalling of the mortar took place. These widening cracks coalesced into a single longitudinal crack as the samples split longitudinally. The properties of mortar obtained from the compression tests are given in Table 5.

5.5. Mortar under flexure

Under flexure it can be seen that the specimens ultimately fail due to a transverse crack along the width in the central portion. The load–deflection plots for mortar under flexure are shown in Fig. 10. Mortar modulus was estimated using elementary theory of beams i.e.

$$E = \frac{Pl^3}{48\delta I}, \tag{1}$$

where P is the load, l is the effective span of the specimen, δ is the central deflection and I is the gross moment of inertia. The values of the moduli obtained are listed in Table 6. It may be noted that these values are in between the compression and tension moduli obtained from the in-plane tests (Tables 4 and 5). For the mortar specimens the flexural strength was found to increase with the thickness. In all the specimens cracking was initiated on the bottom face. All failures were sudden and brittle.

Table 5
Properties of mortar under in-plane compression

Category designation	C4
Elastic modulus (MPa)	7100
Stress at first deviation from linearity (MPa)	7.81
Ultimate stress (MPa)	12.8
Strain at failure	0.006

Table 6
Mortar modulus obtained from flexure tests

Category designation	Overall dimensions (mm)	Elastic modulus (MPa)
F2	237 × 60 × 9	5945
F3	237 × 60 × 14	6020
F4	237 × 60 × 19	6105
F5	237 × 60 × 24	5990
F6	237 × 60 × 29	6063

5.6. Ferrocement under in-plane tension

From the tests conducted, it is observed that the first crack develops at the top and bottom mortar layer in the width direction of the sample (Fig. 4). The subsequent increase in the load results in the propagation of the cracks to the middle mortar layers and the widening of cracks at the outermost mortar faces. When the load is increased further, the number of cracks increase followed by chipping and spalling of the mortar portions. When the mortar fails completely the load is taken up by the meshes which start yielding with further increase in the load. The linear first stage ceases with the cracking of the mortar. In the second stage the load carrying capacity of the mortar decreases and the meshes start taking most of the load. Finally in the third stage meshes start yielding. The bond between mortar and the rein-

forcement is subsequently lost. The smoothened load–displacement plots are shown in Figs. 11–13.

The number of mesh layers were varied (along with thickness of the section) from 3 to 5 for ferrocement plates with woven mesh. The results derived from these tests are given in Table 7 and the smoothened load–displacement plots are shown in Fig. 11. It is observed

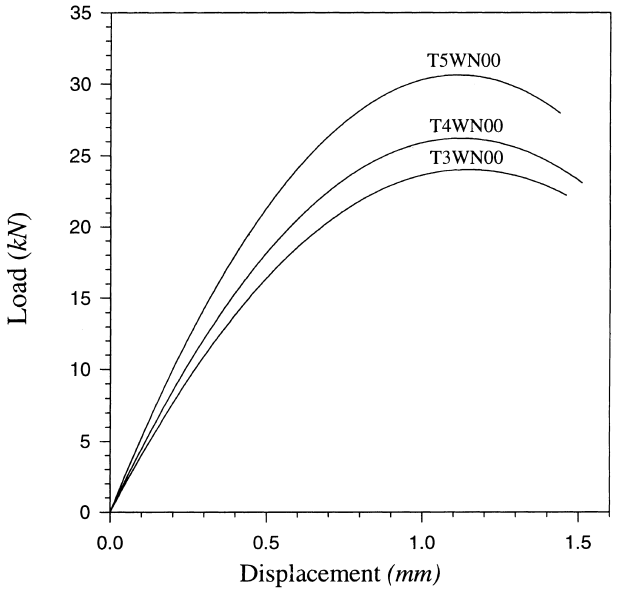

Fig. 11. Load–displacement curves for woven mesh ferrocement specimens with varying number of mesh layers tested under in-plane tension.

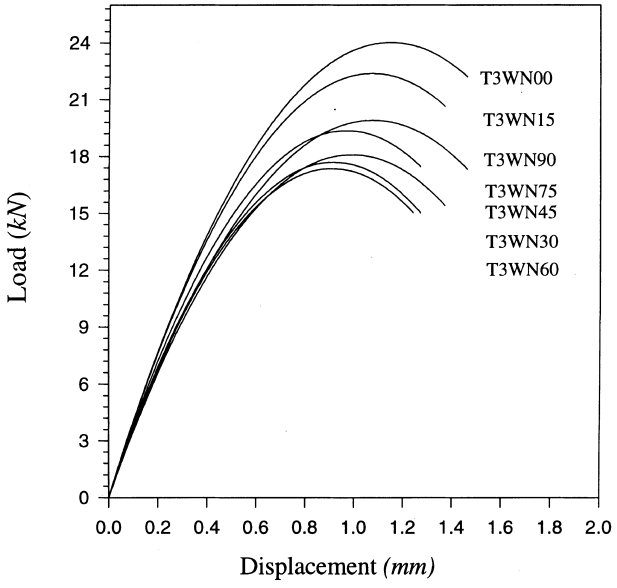

Fig. 12. Load–displacement curves for woven mesh ferrocement specimens with varying mesh orientation, tested under in-plane tension.

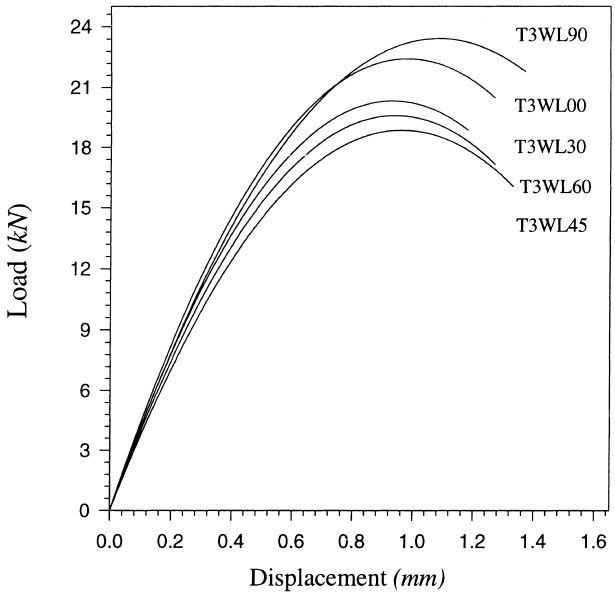

Fig. 13. Load–displacement curves for welded mesh ferrocement specimens with varying mesh orientations, tested under in-plane tension.

that the tensile load carrying capacity of the section increases with the increasing layers of wire mesh. However, since the thickness of the section was also increased the Young's moduli of the composite are not significantly altered. Table 7 indicates an excellent similarity of results in the initial linear range of samples of different thickness.

The load–displacement plots for specimens with woven mesh at different orientations are shown in Fig. 12 and the properties derived from the tests are given in Table 8. From the experimental results the weakest configuration in terms of elastic modulus, stress at first deviation from linearity and ultimate yield stress, is when the mesh orientation is between 30° and 60°. It may be noted that of the mesh orientations selected, the 45° orientation results in the lowest volume fraction of wire mesh in the direction of loading. For a square mesh one would expect to obtain similar results for 15° and 75° orientations and also for 30° and 60° orientations. However, the woven mesh employed was rectangular, which resulted in an identical volume fraction when the direction of loading was at 15° and 90° to the mesh orientations. The similarity of some results for these two cases can be observed in Table 8. A definite trend can be observed in the elastic properties with the change of orientation. Similarly it appears that a change in the volume fraction in the longitudinal direction influences the ultimate load carrying capacity of the specimens.

In-plane tension tests were also conducted on specimens with welded meshes at different orientations. The results obtained from these are given in Table 9 and the load–displacement plots are shown in Fig. 13.

Table 7
Properties of ferrocement specimens with woven mesh and varying mesh layers under in-plane tension

Category	T3WN00	T4WN00	T5WN00
Number of mesh layers	3	4	5
Orientation	0°	0°	0°
Thickness (mm)	24	30	36
Volume fraction in longitudinal direction	0.0078	0.0084	0.0085
Volume fraction in transverse direction	0.0068	0.0072	0.0073
Load at first deviation from linearity (kN)	13.6	17.3	20.7
Ultimate yield load (kN)	23.5	25.1	29.6
Elastic modulus (MPa)	5440	5530	5560
Uniaxial stress at first deviation from linearity (MPa)	10.9	11.1	11.1
Ultimate yield stress (MPa)	18.8	16.1	15.8

Table 8
Properties of ferrocement specimens with woven mesh and varying orientation under in-plane tension

Category	T3WN00	T3WN15	T3WN30	T3WN45	T3WN60	T3WN75	T3WN90
Number of mesh layers	3	3	3	3	3	3	3
Orientation	0°	15°	30°	45°	60°	75°	90°
Thickness (mm)	24	24	24	24	24	24	24
Volume fraction in longitudinal direction	0.0078	0.0068	0.0048	0.0037	0.0043	0.0060	0.0068
Volume fraction in transverse direction	0.0068	0.0060	0.0043	0.0037	0.0048	0.0068	0.0078
Load at first deviation from linearity (kN)	13.6	13.5	13.1	12.9	13.0	13.3	13.5
Ultimate yield load (kN)	23.5	21.6	16.4	16.7	16.2	18.7	18.6
Elastic modulus (MPa)	5440	5409	5238	5148	5207	5340	5401
Uniaxial stress at first deviation from linearity (MPa)	10.9	10.8	10.5	10.3	10.4	10.7	10.8
Ultimate yield stress (MPa)	18.8	17.3	13.1	13.4	13.0	15.0	14.9

Behaviour similar to specimens with woven mesh is observed for those with welded mesh with regard to the weakest configuration. However, due to square openings a fairly close matching is observed for 0° and 90° orientations and also for 30° and 60° orientations. The ultimate yield stress for ferrocement with welded meshes was not found to be higher than that for woven wire meshes in spite of significantly higher volume fractions. This is perhaps because of inferior reinforcement material used for these meshes. This was also reflected in the tests conducted on mesh specimens. Another reason for the low values is that the mesh openings are larger for welded meshes which results in poorer bonding and confining characteristics. Decreasing levels of the ultimate yield load are obtained as the orientation is increased from 0° to 45°.

5.7. Ferrocement under in-plane compression

The load–displacement plots for ferrocement specimens tested under compression is shown in Fig. 14. From the tests, the general material behaviour is observed to be the same as reported in literature [6]. As the load was increased cracks developed in the mortar layers

Table 9
Properties of ferrocement specimens with welded mesh and varying orientation under in-plane tension

Category	T3WL00	T3WL30	T3WL45	T3WL60	T3WL90
Number of mesh layers	3	3	3	3	3
Orientation	0°	30°	45°	60°	90°
Thickness (mm)	24	24	24	24	24
Volume fraction in longitudinal direction	0.0136	0.0085	0.0068	0.0085	0.0136
Volume fraction in transverse direction	0.0136	0.0085	0.0068	0.0085	0.0136
Load at first deviation from linearity (kN)	15.4	14.2	13.7	14.1	15.4
Ultimate yield load (kN)	21.6	19.6	17.5	18.5	23.1
Elastic modulus (MPa)	6180	5668	5492	5660	6168
Uniaxial stress at first deviation from linearity (MPa)	12.36	11.3	11.0	11.3	12.3
Ultimate yield stress (MPa)	17.3	15.7	14.0	14.8	18.5

which became wider as the loads were increased. Chipping and spalling of the mortar was also noticed. The crack formation was in the form of a wedge starting at the grip ends and in the longitudinal section of the specimens as shown in Fig. 5. After the formation of the complete wedge, buckling of the meshes is initiated. This is taken as the ultimate yield state. The results obtained are shown in Table 10. It is seen that the modulus of elasticity is higher for compression as compared to that for tension. This is apparently due to higher mortar modulus in compression and due to the confining properties of reinforcement.

5.8. Ferrocement under flexure

The load–deflection plots for ferrocement specimens tested under flexure are shown in Figs. 15–17. In all these tests deflection was measured at the centreline i.e. the line of loading. It was observed that the linear first stage ceases with the initiation of cracking in mortar on the tension face. The load carrying capacity of the specimens, however, continues to increase. This is apparently because the meshes start carrying additional loads. With a load increment the mortar layer above the lower most mesh also starts cracking. At this stage cracks are also observed on the top most mortar layer.

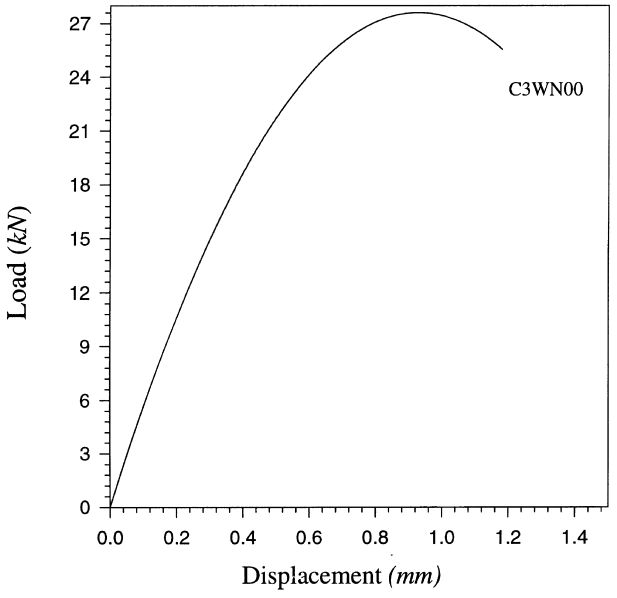

Fig. 14. Load–displacement curve for woven mesh ferrocement specimens tested under in-plane compression.

Table 10
Properties of ferrocement specimens with woven mesh under in-plane compression

Category	C3WN00
Number of mesh layers	3
Orientation	0°
Thickness (mm)	24
Volume fraction in longitudinal direction	0.0078
Volume fraction in transverse direction	0.0068
Load at first deviation from linearity (kN)	20.2
Ultimate yield load (kN)	27.0
Elastic modulus (MPa)	7600
Uniaxial stress at first deviation from linearity (MPa)	16.2
Ultimate yield stress (MPa)	21.6

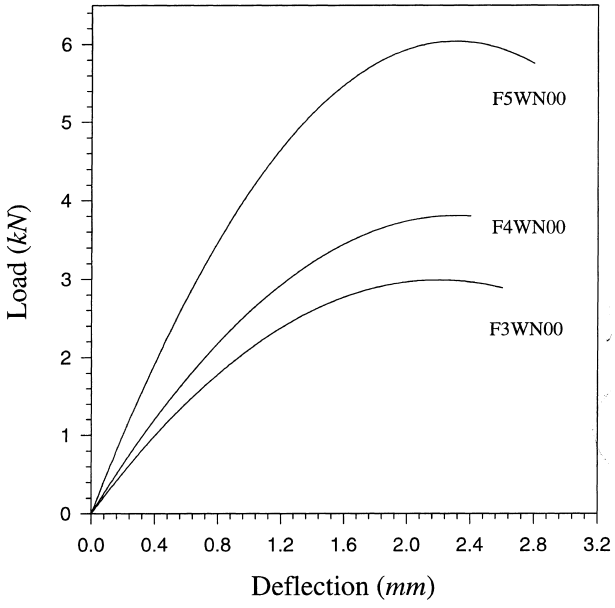

Fig. 15. Load–deflection curves for woven mesh ferrocement specimens with varying number of mesh layers under flexure.

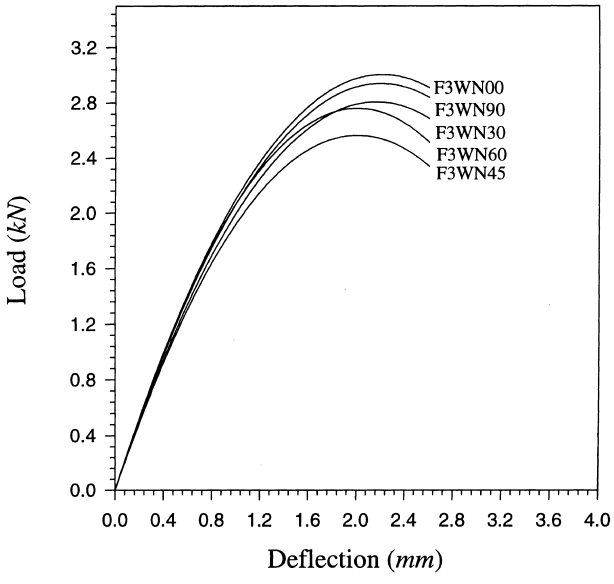

Fig. 16. Load–deflection curves for woven mesh ferrocement specimens with varying mesh orientations under flexure.

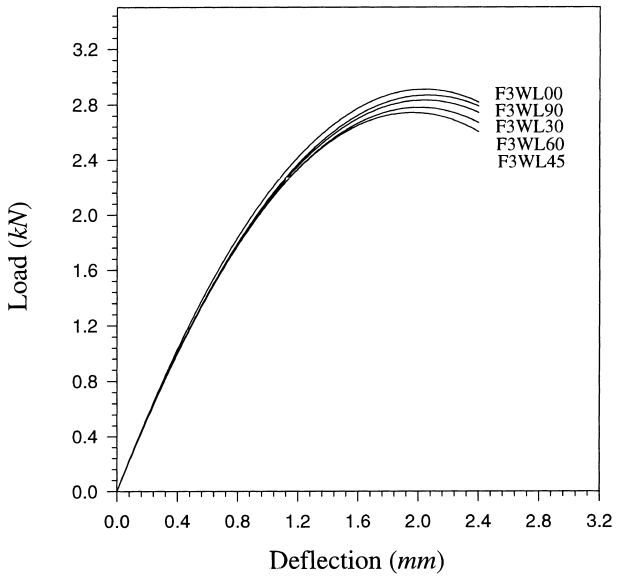

Fig. 17. Load–deflection curves for welded mesh ferrocement specimens with varying mesh orientations under flexure.

Subsequent cracking is due to the propagation of cracks from bottom as well as from the top. All cracks develop in the width direction in central portion of the specimens (Fig. 6). The load–deflection behaviour of ferrocement plates in flexure is similar to that reported in literature [2,4,5].

For the ferrocement plates with woven mesh the number of mesh layers were varied from 3 to 5 layers. It is observed that the flexural strength of the section increases with the increasing number of wire mesh layers (Fig. 15). This is due to the increased thickness of the specimens and the increased depth of mesh layers from the neutral axis.

When the number of layers is kept constant and the mesh orientation is changed it is found that the strongest configuration in both elastic and inelastic ranges results from 0° orientation whereas the weakest configuration results from 45° orientation. The reason for this is the lowest volume fraction in the direction of maximum principal stress, at this orientation. This is so for the samples with woven as well as welded meshes.

6. Mortar modulus determination strategies

A comparison of the mortar moduli obtained from in-plane tension and compression tests was made with those determined from the empirical relations [7,11] using compressive strength tests on mortar cubes and cylinders. The mortar modulus obtained from different relations [10, 12–16] and from the experimental tests are listed in Table 11. These empirical relations have been suggested for concrete and mortar.

It can be seen that various relationships result in a mortar modulus in the range of 16600–30100 MPa, which is a wide range. It should be noted that relations at S. Nos. 7–9 of Table 11 have been proposed specifically for mortar. However, these also yield an extremely high value for mortar modulus as compared to those obtained using in-plane tension and compression tests. The values obtained from in-plane tension and compression tests compare well with the range of mortar modulus values back calculated by the authors [7,11] from experiments on slabs of various investigators.

The limitations of the relations in Table 11 have been recognised by investigators in past as well who have opined that no definite relationship exists between modulus of elasticity and compressive strength [12]. As

Table 11
Mortar moduli from empirical relationships

S.No.	Reference	Method/relationship for mortar modulus	Units for relationship	Mortar modulus E_m (MPa)
1.	ACI 318 (1995) [13]	$E_m = 57600\sqrt{f'_c}$	psi	21330
2.	ACI 318 (1995) [13]	$E_m = (w_c)^{1.5} \times 33\sqrt{f'_c}$	psi	16740
3.	CEB-FIP (1991) [14]	$E_m = 2.15 \times 10^4 \left(\frac{f_{cm}}{10}\right)^{1/3}$	MPa	30120
4.	Mehta and Monteiro (1993) [12]	$E_m = \alpha_e \times (w_c)^{1.5} \times 33\sqrt{f'_c}$	psi	16740
5.	Mehta and Monteiro (1993) [12]	$E_m = \alpha_e \times 2.15 \times 10^4 \left(\frac{f_{cm}}{10}\right)^{1/3}$	MPa	30120
6.	IS:456-1978 [10]	$E_m = 5700\sqrt{f_{ck}}$	MPa	25170
7.	Sahlin (1971) [15]	$E_m = 1000 f_{ck}$	MPa	19500
8.	Sahlin (1971) [15]	$E_m = 1.8 \times 10^6 + 500 f_{ck}$	psi	22400
9.	Bhandari (1982) [16]	$E_m = 757 f_{ck} + 4.9 f_{ck}^2$	MPa	16630
10.	Arif (1997) [7]	In-plane tension tests	MPa	5070
11.	Arif (1997) [7]	In-plane compression tests	MPa	7100
12.	Arif (1997) [7]	Flexural tests	MPa	6025

Characteristic compressive strength of mortar: Cubes $f_{ck} = 19.5$ MPa (2774 psi); Cylinders $f'_c = 18.2$ MPa (2592 psi).
Density of mortar $w_c = 20.2$ kN/m^3 (126.10 lb/ft^3).
Average compressive strength of mortar $f_{cm} = f_{ck} + 8 = 27.50$ MPa.
Factor governing aggregate type $\alpha_e = 1$.

mortar modulus is a critical parameter with regard to the evaluation of composite moduli, its determination through appropriate tests is essential. For a good estimate experimental tests should be aimed towards finding elastic moduli and not compressive strengths.

Mortar has different moduli in tension and compression. For analysis, however, it is more convenient to use a single value of modulus rather than defining different moduli for different loading regimes. A weighted average of the form

$$E_m = \beta E_{mt} + (1-\beta)E_{mc}, \quad (2)$$

where E_{mt} and E_{mc} are moduli obtained from in-plane tension and compression tests respectively, can be utilised. The factor β may vary from 0 to 1.

7. Validation of the rule of mixtures for ferrocement

The rule of mixtures is often used to evaluate the elastic properties of ferrocement. The Voigt model, commonly referred to as direct rule of mixtures, expresses composite modulus as the summation of contributions from matrix and fibres [17] and is expressed as

$$E_c = E_m V_m + E_f V_f, \quad (3)$$

where E and V represent Young's moduli and volume fraction. The subscripts c, m and f refer to composite (ferrocement), matrix (mortar) and fibre (mesh). To account for the weave, geometrical properties and other manufacturing defects, the global effectiveness factor η was introduced [18] and Eq. (3) was modified as

$$E_c = E_m V_m + \eta E_f V_f. \quad (4)$$

A comparison of the Young's elastic modulus obtained using Eqs. (3) and (4) is made with the tests conducted on ferrocement plates. The results are given in Table 12. The moduli for mesh and mortar used in the above equation were the average values obtained in Tables 3 and 4. The volume fractions for the specimens were as given in Tables 7–9.

It is clear from Table 12, that the rule of mixtures predicts the composite modulus in a better way when $\eta = 0.5$ than when $\eta = 1$. This strengthens the fact that the pitch of the weave and the production process affects the fibre contribution to the composite modulus. In general the rule of mixtures yields values of moduli which are fairly close to the values obtained experimentally from tests on ferrocement samples.

As the number of layers of woven wire mesh increases the composite modulus increases due to the increased fibre volume fraction. For the varying orientation of woven and welded wire mesh the lowest composite modulus is encountered at 45° due to the reduction in fibre volume fraction. Similar results have been reported for rectangular slabs by other investigators [2,3]. The composite modulus decreases as the orientation varies from 0° to 45°. It increases as the orientation changes from 45° to 90°. For ferrocement samples with woven mesh, due to the rectangular opening, highest modulus is observed at 0° orientation due to the highest volume fraction. For samples with welded mesh, due to square opening highest modulus is obtained at both 0° and 90° orientations.

Table 12
Validation of rule of mixtures for ferrocement composite modulus

Category	Mesh type	Fibre volume fraction in longitudinal direction	Composite modulus in tension (MPa)		
			As per Eq. (4)		Exp.
			$\eta = 1.0$	$\eta = 0.5$	
T3WN00	Woven	0.0078	5727	5379	5440
T3WN15	Woven	0.0068	5643	5339	5409
T3WN30	Woven	0.0048	5474	5260	5238
T3WN45	Woven	0.0037	5382	5217	5148
T3WN60	Woven	0.0043	5432	5240	5207
T3WN75	Woven	0.0060	5576	5308	5340
T3WN90	Woven	0.0068	5643	5339	5401
T4WN00	Woven	0.0084	5778	5403	5530
T5WN00	Woven	0.0085	5786	5407	5560
T3WL00	Welded	0.0136	6519	5760	6180
T3WL30	Welded	0.0085	5976	5501	5668
T3WL45	Welded	0.0068	5795	5415	5492
T3WL60	Welded	0.0085	5976	5501	5660
T3WL90	Welded	0.0136	6519	5760	6168

Mortar modulus in tension = 5070 MPa.
Fibre modulus for woven mesh = 89312 MPa.
Fibre modulus for welded mesh = 111641 MPa.

8. Conclusions

A range of elastic and inelastic properties were evolved from experiments on ferrocement and its constituents. It is hoped that these properties and load–displacement response trends will contribute in the analytical simulation of ferrocement behaviour.

The tests on mortar indicate that the conventional empirical relations based predominantly on the mortar crushing strength, considerably overestimate the mortar modulus. The elastic moduli evaluated for ferrocement specimens using the rule of mixtures compare well with the moduli obtained from tests. The change of composite modulus due to the change in orientation of meshes is implicit in the rule of mixtures. This trend was also observed in the experiments. The 45° orientation emerges as the weakest configuration because of the lowest volume fraction of wire mesh in the direction of loading at this orientation.

From the flexural tests on mortar specimens, the mortar modulus was evaluated using bending theory and was found to be close to the average moduli obtained from in-plane tension and compression tests. The flexural tests undertaken on the ferrocement specimens with woven and welded mesh showed that the weakest configuration is encountered at 45° orientation.

Acknowledgements

The authors sincerely acknowledge the financial assistance received vide CSIR grant no. 70(0003)/93/EMR-I, Govt. of India. Helpful discussions with Prof. S. Basu and Prof. S. Ray of University of Roorkee are gratefully acknowledged. All the experiments were conducted at the University of Roorkee. The help extended by the staff is gratefully acknowledged.

References

[1] Nervi PL. Structures. New York: F.W. Dodge, 1956.
[2] Johnston CD, Mowat DN. Ferrocement material behaviour in flexure. ASCE, J Structural Division 1974;100:2053–69.
[3] Johnston CD, Mattar SG. Ferrocement behaviour in tension and compression. ASCE, J Structural Division 1976;102:875–89.
[4] Balaguru PN, Naaman AE, Shah SP. Analysis and behaviour of ferrocement in flexure. ASCE, J Structural Division 1977;103:1937–51.
[5] Paramasivam P, Ravindrarajah RS. Effect of arrangement of reinforcements on mechanical properties of ferrocement. ACI Journal 1988;85:3–11.
[6] Rao PK. Stress strain behaviour of ferrocement elements under compression. J Ferrocement 1992;22:343–52.
[7] Arif M. Simulation of the Mechanical Properties of Ferrocement Plates. Ph.D thesis, Roorkee: University of Roorkee, 1997.
[8] IS: 269-1989. Indian Standard Specifications for Ordinary or Low Heat Portland Cement. Bureau of Indian Standards, New Delhi: 1989.
[9] ACI Committee 549 1R-88. Guide for the design, construction and repair of ferrocement. ACI Structural Journal, May–June 1988.
[10] IS: 456-1978. Code of Practice for Plain and Reinforced Concrete. Bureau of Indian Standards, New Delhi: 1978.
[11] Pankaj, Arif M, Kaushik SK. Mortar modulus for ferrocement: a state of uncertainty. J Ferrocement 1996;17:313–20.
[12] Mehta PK, Monteiro PJM. Concrete, Structure, Properties and Materials. Englewood Cliffs, NJ: Prentice-Hall, 1993.
[13] ACI-318. Building Code Requirements for Reinforced Concrete. American Concrete Institute, Detroit: 1995.
[14] CEB-FIP Model Code. International Recommendations for the Design and Construction of Concrete Structures. Comité Euro-International du Béton, Paris, France: 1991.
[15] Sahlin S. Structural Masonry. Englewood Cliffs, NJ: Prentice-Hall, 1971.
[16] Bhandari NM. Strength of Low Rise Brick Masonry Construction. Ph.D thesis, Roorkee: University of Roorkee, 1982.
[17] Jones RM. Mechanics of Composite Materials. New York: Mc-Graw Hill, 1975.
[18] Huq S, Pama RP. Ferrocement in tension: analysis and design. J Ferrocement 1978;8:143–67.